

TCEB1-mutated renal cell carcinoma: a distinct genomic and morphological subtype

A Ari Hakimi^{1,2,9}, Satish K Tickoo^{3,9}, Anders Jacobsen^{4,9}, Judy Sarungbam³, John P Sfakianos¹, Yusuke Sato^{5,6}, Teppei Morikawa⁷, Haruki Kume⁵, Masashi Fukayama⁷, Yukio Homma⁵, Ying-Bei Chen³, Alexander I Sankin¹, Roy Mano¹, Jonathan A Coleman¹, Paul Russo¹, Seishi Ogawa⁶, Chris Sander⁴, James J Hsieh^{2,8,9} and Victor E Reuter^{3,9}

¹Department of Surgery—Urology Service, Memorial Sloan Kettering Cancer Center, New York, NY, USA;

²Human Oncology and Pathogenesis Program, Memorial Sloan Kettering Cancer Center, New York, NY, USA;

³Pathology, Memorial Sloan Kettering Cancer Center, New York, NY, USA; ⁴Computational Biology, Memorial Sloan Kettering Cancer Center, New York, NY, USA; ⁵Department of Urology, Graduate School of Medicine, University of Tokyo, Tokyo, Japan;

⁶Department of Tumor Biology, Graduate School of Medicine, Kyoto University, Kyoto, Japan; ⁷Department of Pathology, Graduate School of Medicine, University of Tokyo, Tokyo, Japan and ⁸Medicine, Memorial Sloan Kettering Cancer Center, New York, NY, USA

Integrated sequencing analysis identified a group of tumors among clear cell renal cell carcinomas characterized by hotspot mutations in *TCEB1* (a gene that contributes to the *VHL* complex to ubiquitinate hypoxia-inducible factor). We analyzed 11 tumors from two distinct cohorts with *TCEB1* mutations along with an expanded cohort to assess whether these should be considered an entity distinct from clear cell renal cell carcinoma and clear cell papillary renal cell carcinoma. All tumors were characterized by hotspot mutations in *TCEB1* Y79C/S/F/N or A100P. Morphological and immunohistochemical characteristics of the tumors were assessed by two experienced genitourinary pathologists. Clinical and pathological variables, copy number alterations, mutations, and expression signatures were compared with a cohort of *TCEB1* wild-type tumors. All *TCEB1*-mutated tumors were *VHL* and *PBRM1* wild type and contained distinct copy number profiles including loss of heterozygosity of chromosome 8, the location of *TCEB1* (8q21.11). All tumors lacked the clear cell renal cell carcinoma signature 3p loss and contained distinct gene expression signatures. None of the clear cell papillary tumors harbored *TCEB1* mutations. Pathologically, all *TCEB1*-mutated tumors shared characteristic features including thick fibromuscular bands transecting the tumor, pure clear cell cytology frequently with cells showing voluminous cytoplasm, and clear cell renal cell carcinoma-like acinar areas associated with infolding tubular and focally papillary architecture. The presence of voluminous cytoplasm, absence of luminal polarization of tumor nuclei, and lack of extensive cup-like distribution of carbonic anhydrase-IX expression distinguish it from clear cell papillary carcinoma. None of the patients developed metastases at last follow-up (median 48 months). In sum, *TCEB1*-mutated renal cell carcinoma is a distinct entity with recurrent hotspot mutations, specific copy number alterations, pathway activation, and characteristic morphological features. Further clinical follow-up is needed to determine whether these tumors are more indolent compared with the conventional clear cell renal cell carcinoma.

Modern Pathology (2015) **28**, 845–853; doi:10.1038/modpathol.2015.6; published online 13 February 2015

Renal cell carcinoma is a broad term encompassing multiple different malignant subtypes arising from the kidney with various histopathological appearances, molecular alterations, and clinical outcomes.

Correspondence: Dr AA Hakimi, MD, Department of Surgery, Urology Service, 353 E 68th St, New York, NY 10065, USA.

E-mail: hakimia@mskcc.org

⁹These authors contributed equally to this work.

Received 13 October 2014; revised 5 December 2014; accepted 5 December 2014; published online 13 February 2015

For the past several decades, tumor subtyping primarily relied on morphological and immunohistochemical characterization, recognizing tumors including the most common and aggressive, clear cell renal cell carcinoma, as well as papillary and chromophobe subtypes.¹ Nevertheless morphological overlap is common and unique classes of tumors are now being recognized from within these classic subtypes. Clear cell papillary renal cell carcinoma exemplifies now a well-recognized entity with unique growth pattern characteristics

and immunohistochemical features that has been distinguished from the clear cell renal cell carcinoma group.² At the same time, while clear cell renal cell carcinoma and clear cell papillary renal cell carcinoma tumors are morphologically distinct tumors, they share common activation of hypoxia-inducible factor (HIF) pathway.

Several large-scale molecular and genomic studies including the ongoing work by the Cancer Genome Atlas (TCGA) have further refined these morphological subtypes. Exome and copy number analysis has shown loss of 3p and *VHL* mutations to be the fundamental events in carcinogenesis of clear cell renal cell carcinoma.^{3,4} More recent work has identified *PBRM1* as the next most commonly mutated gene (~30–60%).^{3,5,6} Additional loss of multiple 3p tumor suppressors is common in clear cell renal cell carcinoma and often correlates with disease aggressiveness.^{7,8}

Sato *et al*⁴ recently identified a group of tumors within clear cell renal cell carcinoma that lacked the characteristic 3p loss and *VHL* mutations. These tumors were defined by the loss of heterozygosity on chromosome 8q along with characteristic transcription elongation factor B (*TCEB1*) hotspot mutations, affecting the binding site of *VHL* and thus the ability to ubiquitinate the HIF complex. These tumors may suggest a novel mechanism for the origin of a group of clear cell renal cell carcinoma that does not involve the loss of *VHL*. We hypothesize that they may represent a distinct tumor entity and utilized the rich genomic, pathological, and clinical data from two distinct datasets, Sato *et al* and TCGA, to further investigate.

Materials and methods

Genomic Data

Publicly available genomic data for the Sato *et al* and TCGA datasets were acquired. The Sato *et al* cohort consisted of 8, mostly low-grade tumors with *TCEB1* mutation. Five out of the eight tumors had whole-exome sequencing data and mRNA gene expression array data, and the remaining three tumors had targeted deep DNA sequencing data available. All 8 tumors contained SNP array copy number data. An additional 67 low-grade (Fuhrman nuclear grade 1 and 2) tumors had SNP array copy number and mRNA expression data available (ArrayExpress accession number 'E-MTAB-1980'). We chose low-grade tumors in a comparison group given that *TCEB1*-mutated tumors are mostly low grade and appear to have an indolent clinical behavior, and thus attempted to avoid spurious findings related to more aggressive tumors.

In the TCGA cohort, three *TCEB1*-mutated tumors were identified, all of which had whole-exome sequencing, copy number, and mRNA expression data (RNA-seq) available. To draw statistical genomic

comparisons with clear cell renal cell carcinoma tumors, similar to that done in Sato *et al* cohort, we also compared *TCEB1*-mutated tumors with low-grade tumors within the TCGA cohort with complete genomic data available ($n=193$; $n=180$ including mRNA expression data). All TCGA datasets were obtained from the Broad FireHose (<http://gdac.broadinstitute.org/>, 16 January 2013 data run).

Comparative Analysis of Tumor Genomic Profiles

To compare *TCEB1* mutant and wild-type tumor genomic profiles, we combined *TCEB1* mutant tumor samples from Sato *et al* and TCGA ($n=11$) and compared these to low-grade TCGA tumors with complete genomic data ($n=193$). We computed genome-wide estimates of DNA copy number gain or loss frequencies in the two tumor sets using the Integrated Genomics Viewer (gain: $\log_2(\text{CN}/2) > 0.1$; loss: $\log_2(\text{CN}/2) < -0.1$). Somatic mutation frequencies in the two tumor sets were computed for all recurrently mutated genes identified in a separately published analysis of the TCGA cohort ($n=15$).³

Gene Expression Analysis

Gene expression profiles of *TCEB1* mutant tumors from the Sato *et al* (Agilent 4x44k microarrays) and TCGA (RNA-seq) cohorts, was performed by computing gene expression changes between *TCEB1*-mutated (Sato: $n=5$, TCGA: $n=3$) and wild-type (Sato: $n=67$, TCGA: $n=180$) tumors separately for each of the two distinct cohorts. The correspondence in gene expression changes between the two cohorts was evaluated by using the Pearson's correlation coefficient (two-tailed *t*-test) and Spearman rank correlation coefficient (two-tailed *t*-test). To combine gene expression profiles from the cohorts, log-expression levels were normalized by using z-scores. For individual genes, we tested changes in expression between *TCEB1*-mutated and wild-type tumors by using the nonparametric Wilcoxon rank-sum test (two-tailed *P*-values).

Gene Set and Pathway Enrichment Analysis

We used Gene Set Enrichment Analysis (GSEA)⁹ to statistically evaluate the extent that particular gene sets or pathways were dysregulated in *TCEB1*-mutated tumors. We analyzed gene expression profiles of $n=5$ mutated vs 67 low-grade clear cell renal cell carcinoma tumors from the Sato *et al* cohort. Genes were sorted by mRNA expression change in *TCEB1* mutant vs wild-type tumors, and GSEA was used to evaluate the null hypothesis that genes in particular gene sets or pathways were not differentially expressed in mutant vs wild-type samples. *P*-values were estimated by sample

phenotype permutations ($n=100$), and we tested 1196 curated gene sets using this approach (MSigDB v 4.0, c2 collection of curated gene sets).

Pathological Analysis

All hematoxylin and eosin slides from the cases of *TCEB1*-mutated renal cell carcinoma from Sato *et al* cohort, as well as all the available digital slides from two of three cases from the TCGA cohort, were reviewed by two experienced genitourinary pathologists (VER and SKT). Additional unstained slides were acquired from the Sato *et al* cohort and immunohistochemical stains for carbonic anhydrase-IX (CA-IX), HIF-1-alpha (HIF-1a), cytokeratin 7 (CK7), CD10, and high molecular weight cytokeratin (34BE12) were performed. The choice of immunohistochemical stains was based on the utility of these markers among certain renal cell carcinomas that may be confused with these *TCEB1*-mutated tumors because of some morphological overlaps.^{2,10}

Available digital slides of clear cell renal cell carcinoma from TCGA web-portal (<https://tcga-data.nci.nih.gov/tcga/>) were reviewed to ascertain if the morphological features of *TCEB1*-mutated tumors are unique, or whether these were shared by some other clear cell renal cell carcinoma tumors.

Results

Copy Number Analysis

As previously reported by Sato *et al*, all of the *TCEB1*-mutated tumors were characterized by broad loss of heterozygosity of chromosome 8, with one tumor (clear cell renal cell carcinoma-42) containing broad copy neutral loss of heterozygosity, one tumor (clear cell renal cell carcinoma-48) containing loss of heterozygosity of most of 8q along with copy neutral loss of heterozygosity of *TCEB1* (Supplementary Figure 1). Additionally, none of the tumors contained 3p loss, 5q amplifications, (one tumor contained whole chromosome 5 gain) 9p or 14q loss, which represent the most common copy number aberrations in clear cell renal cell carcinoma. All three *TCEB1*-mutated tumors in the TCGA demonstrated nearly identical copy number alterations. All tumors contained broad loss of heterozygosity of chromosome 8, and none contained 3p loss, 5q gain, 9p or 14q loss (Figure 1a for comparison with the TCGA cohort). Four of the 11 *TCEB1*-mutated tumors contained broad gains of chromosome 7, but no other recurrent events were noted.

Mutation Analysis

All TCGA *TCEB1* mutations exclusively involved *VHL*-binding site residues Tyr79. The *TCEB1* mutant tumors, as assessed from either Sato *et al* or TCGA

cohorts, had completely different mutation patterns compared with clear cell renal cell carcinoma which show frequently mutated 3p genes including *VHL*, *PBRM1*, or *SETD2* (Supplementary Figure 2). One tumor in the Sato *et al* cohort contained a mutation in *BAP1*; however, this was a missense mutation predicted to have low functional impact, and was not accompanied by 3p loss. Additionally, immunohistochemical staining of this tumor showed a retained *BAP1* protein (data not shown). Further interrogation of both cohorts identified only two recurrent clear cell renal cell carcinoma-associated mutations in the *TCEB1*-mutated samples, a *PIK3CA* mutation (ccrcc-48) and a *MUC4* mutation (ccrcc-35) (Figure 1b).

Expression Analysis

After demonstrating that *TCEB1*-mutated tumors possess a unique copy number and mutation profiles, we hypothesized that these tumors would possess specific expression signatures. We compared the expression profiles of *TCEB1*-mutated tumors with a large number of low-grade *TCEB1* wild-type tumors.

First, we compared the whole transcriptome expression profiles of *TCEB1* mutant tumors from the Sato *et al* and TCGA cohorts ($n=5$ and 3, respectively). Comparing expression changes (measured by microarrays and RNA-seq) between the two cohorts identified a strong global correlation (Spearman correlation $\rho = 0.47$, $P = 0$, Figure 2). This correlation was not due to a bias in DNA copy number profiles, as the same level of correlation ($\rho = 0.46$) was present even after removing all genes on chromosomes with frequent copy number alterations (chromosomes 3, 5, 9, 14, and 8) (data not shown). This result was concordant with our hypothesis that *TCEB1* mutant tumors had unique expression signatures.

Combined dataset pathway-based analysis revealed statistically significant gene expression changes associated with *TCEB1* mutations. Several of the top ranking downregulated gene sets ($P < 0.05$) were associated with *TCEB1* gene function and its role in the formation and activation of RNA polymerase II (POL II) elongation (Supplementary Table 1). Interestingly, *TCEB1*-mutated tumors showed mRNA downregulation of multiple components involved in RNA Pol II elongation such as *TCEB1*, *TCEB2*, *POLR2C*, *POLR2E*, and *CDK7* ($P < 0.05$, TCGA and Sato *et al* data combined, Figures 3a and b). In addition to the *TCEB* mutations, all *TCEB1*-mutated tumors also carried a chromosome 8 loss of heterozygosity (8-loss of heterozygosity) in the other allele. On the other hand, while 25 low-grade clear cell renal cell carcinoma tumors showed an 8-loss of heterozygosity, none had a *TCEB1* mutation. We therefore analyzed expression changes in these tumors separately from other low-grade tumors in

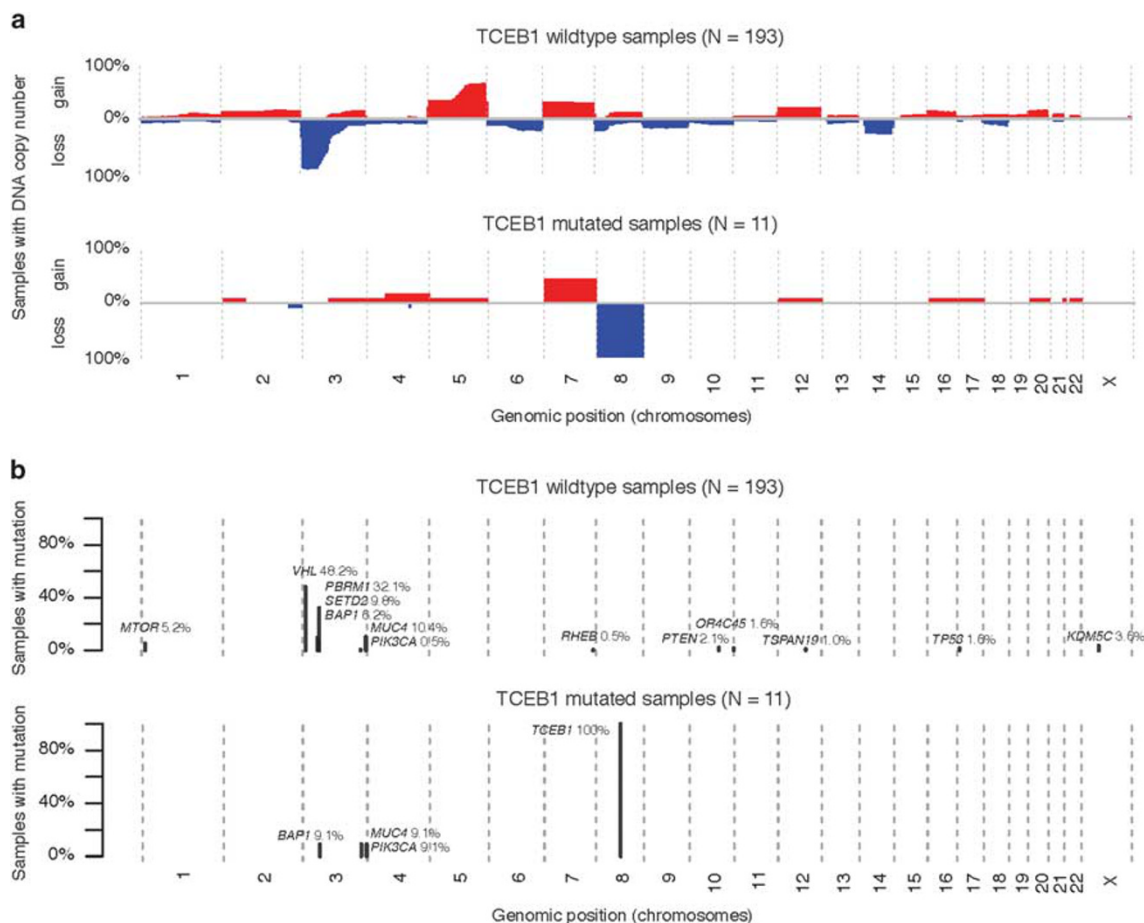


Figure 1 (a) Genome-wide copy number plots depicting chromosomal gains (red) and losses (blue) in low-grade clear cell renal cell carcinoma samples from the Cancer Genome Atlas vs *TCEB1*-mutated samples in the combined the Cancer Genome Atlas and Sato *et al* datasets. (b) Recurrent mutations in both the combined low-grade clear cell renal cell carcinoma cohort vs *TCEB1*-mutated samples.

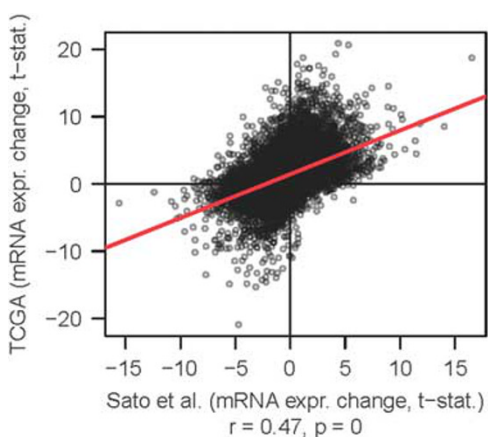


Figure 2 Genome-wide mRNA expression correlation between Sato *et al* and the Cancer Genome Atlas datasets when comparing *TCEB1*-mutated tumors vs low-grade clear cell renal cell carcinoma (X and Y axes, respectively).

order to investigate if the effect on the RNA pol II elongation pathway gene expression levels could be associated to 8-loss of heterozygosity alone.

As expected, *TCEB1* (encoded on chromosome 8) mRNA expression levels were lower in 8-loss of heterozygosity samples compared with other low-grade clear cell renal cell carcinoma tumors (Figure 3b). However, other Pol II elongation pathway genes such as *POLR2C*, *CDK7*, *POLR2E*, and *TCEB2* were significantly downregulated only in the presence of *TCEB1* mutations (Figure 3b).

In summary, these data suggest that *TCEB1* mutations may affect RNA Pol II elongation efficiency by causing a concomitant reduction in the expression of other elongation pathway members through mechanisms unknown at present. Additional intriguing pathway alterations were also noted, most clearly when analyzing the cohorts independently. When analyzing the Sato data set (5 mutated tumors vs 67 low-grade clear cell renal cell carcinomas), several gene sets related to 5' AMP-activated protein kinase (AMPK) pathway activation were downregulated in the *TCEB1*-mutated tumors, suggesting a lack of reliance on the mTOR pathway as compared with clear cell renal cell carcinoma (Supplementary Figure 3). This signal was also evident in the TCGA cohort, although without

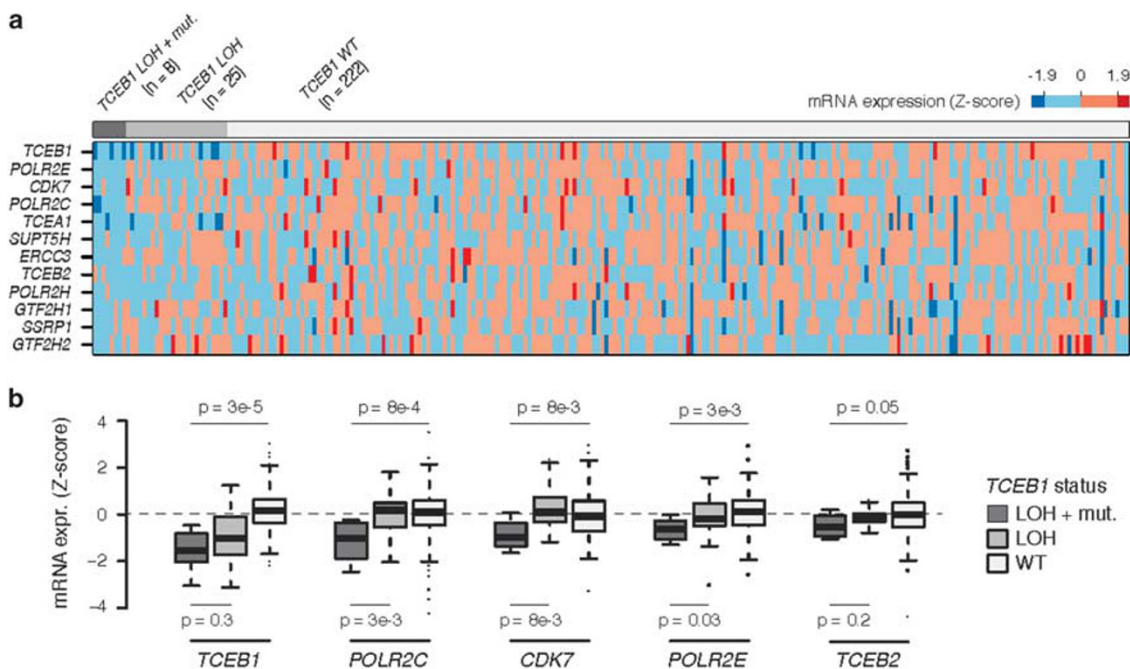


Figure 3 Pathway analysis reveals downregulation of RNA polymerase II elongation genes in *TCEB1*-mutated tumors. (a) Heatmap of mRNA expression of RNA polymerase II elongation genes stratified by *TCEB1* mutation and concomitant loss of heterozygosity (loss of heterozygosity), loss of heterozygosity alone, and in the wild-type setting. (b) Box plot of specific RNA polymerase II elongation genes demonstrating a lack of expression changes in tumors with a loss of heterozygosity alone compared with combined *TCEB1* mutation and loss of heterozygosity.

statistical significance likely related to the smaller cohort (3 mutated tumors vs 180 low-grade clear cell renal cell carcinomas).

Histopathology Results

Microscopic features. All the tumors in which the tumor borders could be assessed (9 of 10) were well-circumscribed with at least a partial encapsulation. Variable amount of cystic change was present in all. All 10 showed thick fibromuscular bands traversing (as well as surrounding at least partially in most cases) the tumor (Figure 4a), imparting a multinodular appearance to the tumor on scanner-view evaluation (Supplementary Figure 4A). Tumor architecture ranged from small acinar with intricately branching thin vascular septations (akin to that seen in a typical clear cell renal cell carcinoma) (Supplementary Figure 4B), to more solid alveolar (Supplementary Figure 4C), tubular (often branching, with infoldings) (Figure 4b), to foci with mostly small papillary tufting or occasional longer papillations (Figure 4c). Cytologically, the tumor cells appeared to have a clear cytoplasm at low-magnification evaluation. At higher magnification, however, these ‘clear’ cells often showed finely granular or reticulate cytoplasm (Figure 4d). All tumors appeared to have voluminous cytoplasm at least in some areas of the neoplasm (Figure 4d). The cell membranes were prominent, particularly in such

areas. The nuclei in 9/10 were low grade (equal to Fuhrman grade 2) with only a few foci showing easily identifiable nucleoli (similar to Fuhrman grade 3) in one. Three tumors showed linear arrangement of the nuclei, away from the basement membrane (mimicking clear cell papillary renal cell carcinoma) (Supplementary Figure 4D), but this arrangement was only focal. No tumor necrosis, lymphovascular invasion, or histiocytes were present in any tumor. All tumors were confined to the renal parenchyma (Table 1 for summary of the morphology).

Except for the 3 tumors with *TCEB1* mutations, none of the other 300 consecutive tumors with digital slides in the TCGA portal that were reviewed, showed morphological features similar to the *TCEB1*-mutated tumors.

Immunohistochemistry. All 8 tumors on which IHC was performed showed a diffuse positivity for CA-IX (membranous, box-like in 100% of cells) (Figure 4e). HIF-1-alpha (nuclear) was diffusely positive in 5 (Supplementary Figure 4E), and showed patchy positivity in 3. CK7 was positive in all 8 tumors (Figure 4f); in 5 tumors immunoreactivity was diffuse, whereas in 3 it was patchy with only 10–15% cells showing any positivity. CD10 was completely negative in 1 and diffusely positive in 1 (75% cells); in the rest it showed only focal positivity (Supplementary Figure 4F). 34BE12 was

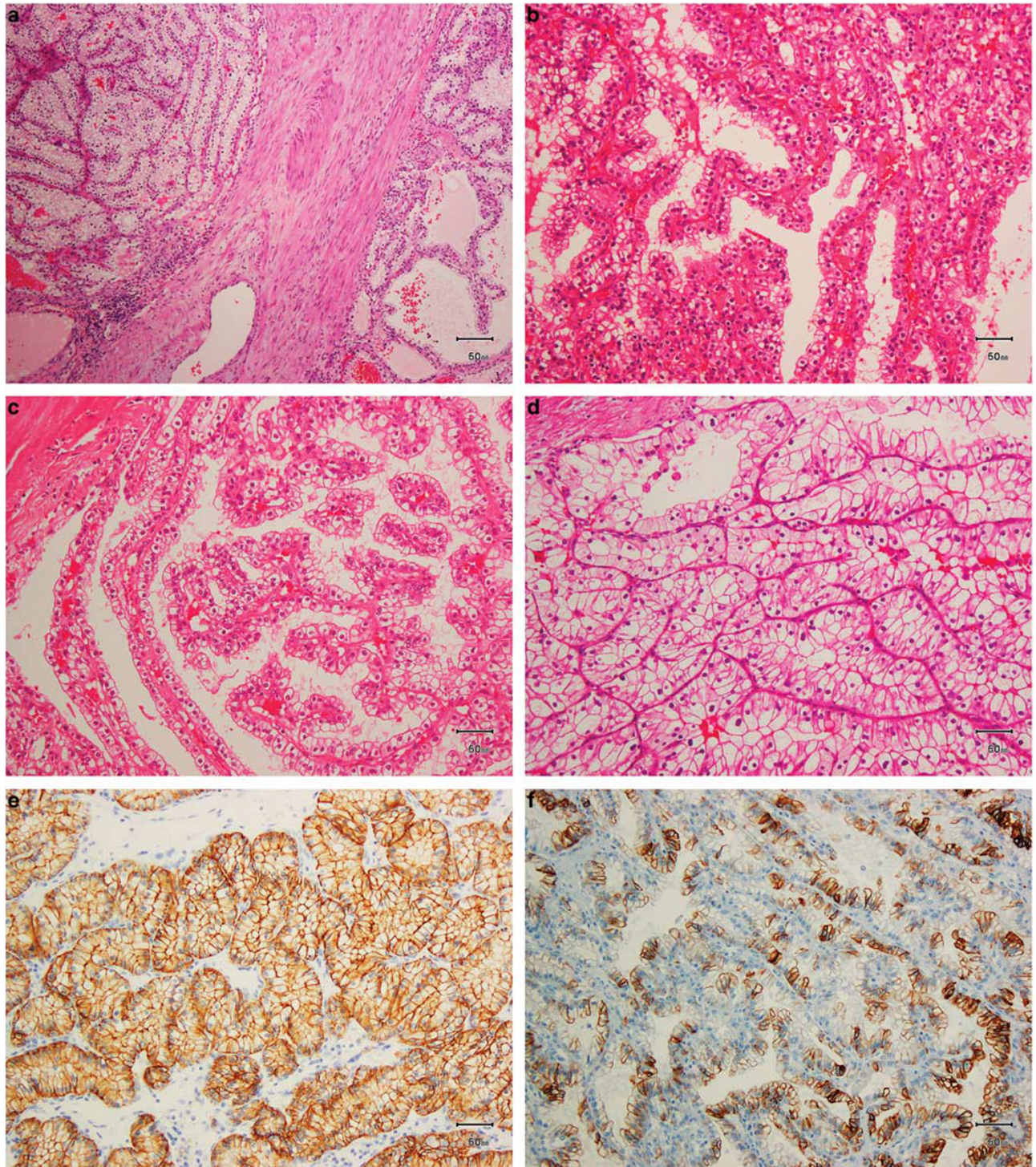


Figure 4 (a) Two nodules of the tumor separated by a thick band of fibromuscular stroma, (b) branching tubules in the tumor; the branchings and infoldings give the appearance of papillations, (c) long, true papillations are also common in the tumor, (d) the clear-appearing cells in the tumor often show fine granules and fibrillations in the cytoplasm; the cells typically appear voluminous with prominent cell membranes, (e) immunohistochemical stain for carbonic anhydrase-IX shows diffuse, membranous (box-like) positivity in all tumors, and (f) all tumors are immunoreactive for cytokeratin 7, exhibiting patchy (as shown here) to more diffuse positivity.

negative in all but 1 tumor, in which very focal staining was observed. See Table 1 for summary.

Molecular comparison. Because some *TCEB1*-mutated tumors showed some features that are

commonly seen in the recently described clear cell papillary renal cell carcinoma (ie, CA-IX, HIF-1, and CK7 positivity, focal linear arrangement of the nuclei, and fibromuscular stroma), we sequenced 10 clear cell papillary renal cell carcinoma tumors,

Table 1 Morphological and immunohistochemical features of *TCEB1*-mutated tumors in the Sato and TCGA datasets

Case #	Fibromuscular bands	Nodular configuration	Architectural patterns (in descending order)*	Clear cells with voluminous cytoplasm and prominent borders	ccPRCC-like nuclear arrangement	HIF-1a (% positive cells)	CA-IX (% positive cells)	CK7 (% positive cells)	CD10 (% positive cells)	34be12 (% positive cells)
1	+	+	TU/BTU, Cystic, Pap	+	–	85	100	60	15	0
2	+	+	TU/BTU, Pap, Acinar, Cystic	+	–	20	100	40	3	0
3	+	+	Cystic, TU/BTU, Acinar	+	+	95	100	75	40	10
4	+	+	Cystic, TU/BTU, Sol alv,	+	–	75	100	10	40	0
5	+	+	Tu/BTU, Cystic, Acinar	+	–	20	100	80	50	0
6	+	+	TU/BTU, Solid alv, Acinar, Cystic, Pap	+	+	70	100	8	0	0
7	+	+	TU/BTU, Cystic, Pap	+	+	35	100	85	20	0
8	+	+	Solid alv, Acinar, TU/BTU, Cystic	+	–	80	100	12	8	0
9	+	+	TU/BTU, Sol alv, Acinar, Cystic, Pap	+	–	ND	ND	ND	ND	ND
10	+	+	Pap, Acinar, Cystic, TU/BTU	+	–	ND	ND	ND	ND	ND

Abbreviations: CA-IX, carbonic anhydrase-IX; ccPRCC, clear cell papillary renal cell carcinoma; HIF-1a, hypoxia-inducible factor-1-alpha; Sol Alv*, solid alveolar; TU/BTU*, tubular, branching tubules. +, present; –, not present; Pap*, true papillations.

Table 2 Clinical and pathological features of *TCEB1*-mutated tumors in the Sato and TCGA datasets

Sample ID	Sex	Age	Stage at diagnosis	Fuhrman grade	Sarcomatoid component	Metastases	Outcome	Follow-up (months)
ccRCC-27	M	56	pT1aN0M0	1	—	—	Alive	53
ccRCC-35	M	67	pT1aN0M0	1	—	—	Alive	46
ccRCC-42	M	73	pT3aN0M0	3	—	—	Alive	39
ccRCC-48	M	42	pT1bN0M0	2	—	—	Alive	33
ccRCC-54	M	57	pT1bN0M0	2	—	—	Alive	40
ccRCC-107	M	66	pT1aN0M0	2	—	—	Alive	106
ccRCC-186	M	60	pT1aN0M0	2	—	—	Alive	48
ccRCC-193	M	77	pT1aN0M0	2	—	—	Alive	85
TCGA-CJ-4889	F	63	pT1aN0M0	Pathology slides unavailable for review	—	—	Alive	64
TCGA-CZ-4862	M	46	pT1bN0M0	2	—	—	Alive	61
TCGA-B8-5545	M	42	pT1aN0M0	2	—	—	Alive	17

Abbreviation: TCGA, the Cancer Genome Atlas.

all of which were found to be wild type for both *TCEB1* and *VHL* (data not shown).

Clinical features. All 11 were pT stage 1 (pT1) tumors, and none has metastasized at last follow-up (median 48 months—Table 2).

Discussion

Detailed comprehensive molecular and pathological analysis of renal cell carcinoma has led to the discovery and expansion of the various renal cell carcinoma subtypes. The latest International Society of Urological Pathology consensus conference on Renal Neoplasms has identified five new distinct renal cell carcinoma entities, including clear cell papillary renal cell carcinoma, acquired cystic disease-associated renal cell carcinoma, and some types of MiTF family translocation associated renal

cell carcinomas.^{1,11,12} Similarly our combination of genomic and pathological interrogation suggests that *TCEB1*-mutated renal cell carcinoma tumors deserve to be added as a novel variant of renal cell carcinoma.

Utilizing a combined cohort of 11 *TCEB1*-mutated tumors, we found a complete lack of the fundamental events of a clear cell renal cell carcinoma carcinogenesis, namely losses of 3p and *VHL*, which have been detected at rates as high as 80–90% in a clear cell renal cell carcinoma.^{3,13,14} Further distinguishing these tumors from the clear cell renal cell carcinoma, they lack secondary alterations in tumor suppressors such as *PBRM1*, and mutations in genes such as *SETD2*, *KDM5C*, and *BAP1*, which predict for aggressive forms of clear cell renal cell carcinoma (one tumor with a *BAP1* missense mutation had no loss of 3p and had retained *BAP1* protein expression on immunohistochemistry). *TCEB1*-mutated tumors also did not possess any

additional recurrent copy number events such as 5q amplifications or 14q or 9p losses that are common in the clear cell renal cell carcinoma. These distinct mutation and copy number profiles were exclusive in the *TCEB1*-mutated samples even when comparing them to a similarly low-grade cohort found in the clear cell renal cell carcinoma TCGA samples, as well as clear cell papillary renal cell carcinoma.

Intriguingly, *TCEB1* mutational patterns do not follow the classical tumor suppressor profile; the mutations almost always occur at a single hotspot amino acid residue (Tyr 79), which would follow more of an oncogene paradigm—although data from Sato *et al* suggests that the region interferes with *VHL* binding. On the other hand, all *TCEB1*-mutated samples were always accompanied by a loss of the companion allele, which is a feature associated with a tumor suppressor. To our knowledge this is the first known example of this phenomenon.

Further evidence of genomic uniqueness of these tumors came from mRNA expression analysis, which was available on 8 tumors. First, unbiased genome-wide analysis showed a strong correlation between differently expressed genes in the *TCEB1*-mutated tumors vs the low-grade TCGA tumors in both independent cohorts. Secondly, pathway-based analysis of expression changes showed strong enrichment in pathways in which *TCEB1* has a vital function. *TCEB1* encodes for the protein elongin C, which is one of three subunits of the factor B (SIII) complex. This entire complex is essential for proteasomal degradation of hydroxylated HIF-1 α through the recruitment of *VHL* and explains how these tumors display overexpressed HIF-1 α and its downstream signaling patterns such as CA-IX (Figure 4e) without loss of *VHL*.^{15,16} This factor also increases the POL II transcription elongation past template-encoded arresting sites.¹⁶ In our

analysis, tumors with *TCEB1* mutations have a downregulation of multiple genes within this complex including *POLR2E*, *POLR2C*, *CDK7*, *TCEA1*, and *TCEB2*, in addition to *TCEB1* (Figure 3). This polygenic phenomenon suggests that mutated *TCEB1*, which is also associated with lower *TCEB1* mRNA expression levels, may also impact a regulatory feedback loop for other genes in the POL II elongation complex. Further pathway analysis suggested that *TCEB1*-mutated tumors may be less dependent on mTOR signaling and other AMPK-related metabolic programming. This certainly requires further investigation in larger cohorts.

Morphological and immunohistochemical analysis also argued for the distinctness of these tumors. All *TCEB1* tumors contained thick fibromuscular bands transecting the tumor, clear cell cytology frequently with cells showing a voluminous cytoplasm and prominent cell membranes, clear cell renal cell carcinoma-like acinar areas, and frequent infolding tubular and focally papillary architecture. Clear cell renal cell carcinoma with prominent fibromuscular stroma with associated CK7 immunoreactivity have been described in the past.^{2,10,17} Many of such tumors have also been reported to lack *VHL* mutations and 3p losses. Some of these are now regarded as the distinct entity of clear cell papillary renal cell carcinoma. It is likely that many others may be the *TCEB1*-mutated tumors as described herein, since specific investigations involving the gene were not performed in these studies. Because of some morphological and immunohistochemical overlap, and an understanding of the molecular profile^{2,15} of clear cell papillary renal cell carcinoma, we also performed targeted sequencing of 10 clear cell papillary renal cell carcinoma tumors for *TCEB1* and *VHL* mutations. All of the clear cell papillary renal cell carcinoma tumors were wild type

Table 3 Comparative features of *TCEB1*-mutated and clear cell papillary renal cell carcinoma

Features	Clear cell papillary renal cell carcinoma	<i>TCEB1</i> -mutated renal cell carcinoma
<i>Morphological</i>		
Fibromuscular bands	May be present	Present in all tumors
Fibromuscular bands imparting a multinodular appearance	No/very uncommon	Present in all tumors
Branching tubules and papillations	Present	Present
Linear arrangement of nuclei away from basement membrane	Always present, diffusely	May be present, focally
Voluminous cytoplasm with prominent cell membranes	Not present	Present at least focally in all tumors
<i>Immunohistochemical</i>		
CK7	Always diffusely positive (in almost 100% cells)	Positive, in variable proportion of cells (not 100% cells)
Carbonic anhydrase-IX	Always diffusely positive, in a cup-shaped pattern (luminal membranes mostly do not stain)	Always diffusely positive, in a box-shaped pattern (all membranes stain)
CD10	Usually negative; rarely, focally positive	Variably positive in most tumors
High molecular weight cytokeratin (34be12)	Positive in a majority of tumors	Usually negative

Abbreviation: CK7, cytokeratin 7.

for both *VHL* and *TCEB1* (data not shown). Table 3 summarizes some of the morphological and immunohistochemical differences between clear cell papillary and *TCEB1*-mutated renal cell carcinomas.

Our analysis of *TCEB1* tumors has broader implications for understanding the natural history of many clear cell renal cell carcinoma tumors. Although *TCEB1*-mutated tumors, clear cell renal cell carcinoma and clear cell papillary renal cell carcinoma, may share the commonality of HIF-1 α activation, only clear cell renal cell carcinoma possesses the ubiquitous 3p loss. Furthermore, *TCEB1* tumors that are mostly low grade, lack the secondary alterations in 3p genes such as *BAP1* and *SETD2*, suggesting that these additive hits may be essential in promoting high grade and potentially metastatic tumors.

Conclusions

In conclusion, we provide multiple areas of evidence that *TCEB1*-mutated renal cell carcinoma are a unique subtype. Although they share similar activation of HIF as seen in both clear cell renal cell carcinoma and clear cell papillary renal cell carcinoma tumors, the mechanism in which this occurs is through distinct means. The lack of 3p loss and associated mutations potentially explains the indolent nature of these tumors and offers insights into the metastatic underpinnings of clear cell renal cell carcinoma.

Acknowledgments

Funded by the Sidney Kimmel Center for Prostate and Urologic Cancers (AAH); J. Randall & Kathleen L. MacDonald Research Fund in Honor of Louis V. Gerstner, Jr (JJH); Tuttle Cancer Research Fund (JJH); Danish Research Council (AJ); MSKCC Center for Translational Cancer Genomic Analysis; and U24 CA143840 (PI Sander).

Disclosure/conflict of interest

There authors declare no conflicts of interest.

References

- 1 Srigley JR, Delahunt B, Eble JN, *et al*. The International Society of Urological Pathology (ISUP) Vancouver Classification of Renal Neoplasia. *Am J Surg Pathol* 2013;37:1469–1489.
- 2 Rohan SM, Xiao Y, Liang Y, *et al*. Clear-cell papillary renal cell carcinoma: molecular and immunohistochemical analysis with emphasis on the von Hippel-Lindau gene and hypoxia-inducible factor pathway-related proteins. *Mod Pathol* 2011;24:1207–1220.
- 3 Cancer Genome Atlas Research N, Analysis working group: Baylor College of MCcreighton CJ, *et al*. Comprehensive molecular characterization of clear cell renal cell carcinoma. *Nature* 2013;499:43–49.
- 4 Sato Y, Yoshizato T, Shiraishi Y, *et al*. Integrated molecular analysis of clear-cell renal cell carcinoma. *Nat Genet* 2013;45:860–867.
- 5 Varela I, Tarpey P, Raine K, *et al*. Exome sequencing identifies frequent mutation of the SWI/SNF complex gene *PBRM1* in renal carcinoma. *Nature* 2011;469:539–542.
- 6 Hakimi AA, Chen YB, Wren J, *et al*. Clinical and pathologic impact of select chromatin-modulating tumor suppressors in clear cell renal cell carcinoma. *Eur Urol* 2013;63:848–854.
- 7 Kapur P, Pena-Llopis S, Christie A, *et al*. Effects on survival of *BAP1* and *PBRM1* mutations in sporadic clear-cell renal-cell carcinoma: a retrospective analysis with independent validation. *Lancet Oncol* 2013;14:159–167.
- 8 Hakimi AA, Ostrovnaya I, Reva B, *et al*. Adverse outcomes in clear cell renal cell carcinoma with mutations of 3p21 epigenetic regulators *BAP1* and *SETD2*: a report by MSKCC and the KIRC TCGA research network. *Clin Cancer Res* 2013;19:3259–3267.
- 9 Subramanian A, Tamayo P, Mootha VK, *et al*. Gene set enrichment analysis: a knowledge-based approach for interpreting genome-wide expression profiles. *Proc Natl Acad Sci USA* 2005;102:15545–15550.
- 10 Martignoni G, Brunelli M, Segala D, *et al*. Renal cell carcinoma with smooth muscle stroma lacks chromosome 3p and *VHL* alterations. *Mod Pathol* 2014;27:765–774.
- 11 Medendorp K, van Groningen JJ, Schepens M, *et al*. Molecular mechanisms underlying the MiT translocation subgroup of renal cell carcinomas. *Cytogenet Genome Res* 2007;118:157–165.
- 12 Ramphal R, Pappo A, Zielenska M, *et al*. Pediatric renal cell carcinoma: clinical, pathologic, and molecular abnormalities associated with the members of the mit transcription factor family. *Am J Clin Pathol* 2006;126:349–364.
- 13 Beroukhim R, Brunet JP, Di Napoli A, *et al*. Patterns of gene expression and copy-number alterations in von-hippel lindau disease-associated and sporadic clear cell carcinoma of the kidney. *Cancer Res* 2009;69:4674–4681.
- 14 Nickerson ML, Jaeger E, Shi Y, *et al*. Improved identification of von Hippel-Lindau gene alterations in clear cell renal tumors. *Clin Cancer Res* 2008;14:4726–4734.
- 15 Kibel A, Iliopoulos O, DeCaprio JA, *et al*. Binding of the von Hippel-Lindau tumor suppressor protein to Elongin B and C. *Science* 1995;269:1444–1446.
- 16 Aso T, Lane WS, Conaway JW, *et al*. Elongin (SIII): a multisubunit regulator of elongation by RNA polymerase II. *Science* 1995;269:1439–1443.
- 17 Michal M, Hes O, Kuroda N, *et al*. Difference between RAT and clear cell papillary renal cell carcinoma/clear renal cell carcinoma. *Virchows Arch* 2009;454:719.

Supplementary Information accompanies the paper on Modern Pathology website (<http://www.nature.com/modpathol>)